Electronic Supplementary Material (ESI) for Journal of Materials Chemistry A.

SUPPLEMENTARY INFORMATION

A MOF-Mediated Strategy for Constructing Human Backbone-like $CoMoS_3$@N-doped Carbon Nanostructures with Multiple Voids as a Superior Anode for Sodium-Ion Batteries

Su Hyun Yang,[†a] Seung-Keun Park,[†b] Jin Koo Kim,[a] and Yun Chan Kang*[a]

[a] *Department of Materials Science and Engineering, Korea University, Anam-dong, Seongbuk-gu, Seoul 136-713, Republic of Korea. E-mail: yckang@korea.ac.kr*

[b] *Department of Chemical Engineering, Kongju National University, 1223-24 Cheonandaero, Seobuk-gu, Cheonan 31080, Republic of Korea*

[†] *These authors contributed equally to this work.*

Characterization

The morphologies and structures of specimen were investigated by microscopic characterization techniques, including scanning electron microscopy (SEM, VEGA3 SBH), and field-emission transmission electron microscopy (FE-TEM, JEM-2100 F). The crystallographic phases of the samples were confirmed through powder X-ray diffraction (XRD, X'Pert PRO), with Cu–K_α radiation ($\lambda = 1.5418$ Å) at the Korea Basic Science Institute (Daegu). Pyris 1 thermogravimetric (TGA) analyzer (Perkin Elmer) was used to confirm the carbon content in the samples, within the temperature range of 30–700 ℃, at a ramp rate of 10 ℃ min^{-1}, in air. Pore size distributions and surface areas of the samples were calculated using the Brunauer-Emmett-Teller (BET) method, with pure N_2 as the adsorbate gas. X-ray photoelectron spectroscopy (XPS, Thermo Scientific K-Alpha) was adopted for characterizing the chemical nature of the samples, and Raman spectroscopy (Jobin Yvon LabRamHR800, excited by a 632.8 nm He/Ne laser) was performed to examine the structure of the carbon in the samples. The Carbon contents of the sample were analyzed elemental analyzer (EA; vario MICRO cube and Cobalt, Molybdenum, and sulfur contents were investigated using the inductively coupled plasma optical emission spectroscopy (ICP-OES; Optima 8300 DV, Perkin Elmer) at the Korea Institute of Ceramic Engineering and Technology (KICET, Jinju).

Electrochemical Measurements

Electrochemical measurement of the $CoMoS_3$@NC, $CoMoS_3$ nanobackbones, MoS_2 tubes, and H-CoS_2 polyhedrons was performed by using standard 2032-type coin half cells. Sodium-ion battery (SIB) anodes were prepared by casting a slurry which included the active material, Super P, and sodium carboxymethylcellulose (weight ratio of 7:2:1, respectively) into DI water, and the mix was then applied onto copper foil, using a doctor blade. All cells were assembled in a glove box, and the coin cell consisted of Na metal as the counter-electrode, porous

polypropylene as the separator, and 1 M $NaClO_4$ (dissolved in a mixture of ethylene carbonate (EC)/dimethyl carbonate (DMC) at a volumetric ratio of 1:1, with addition of 5 wt% fluoroethylene carbonate (FEC)) as the electrolyte. The charge/discharge characteristics and cyclic voltammetry (CV) measurements were performed using a battery analyzer (WonATech, WBCS-3000s cycler) over the potential range of 0.001–3.0 V at various current densities. The diameter of the electrode was 14 mm, and its mass loading was approximately 1.4 mg cm^{-2}. Electrochemical impendence spectroscopy (EIS) analyses were obtained, through the frequency ranges of 0.01–100 kHz.

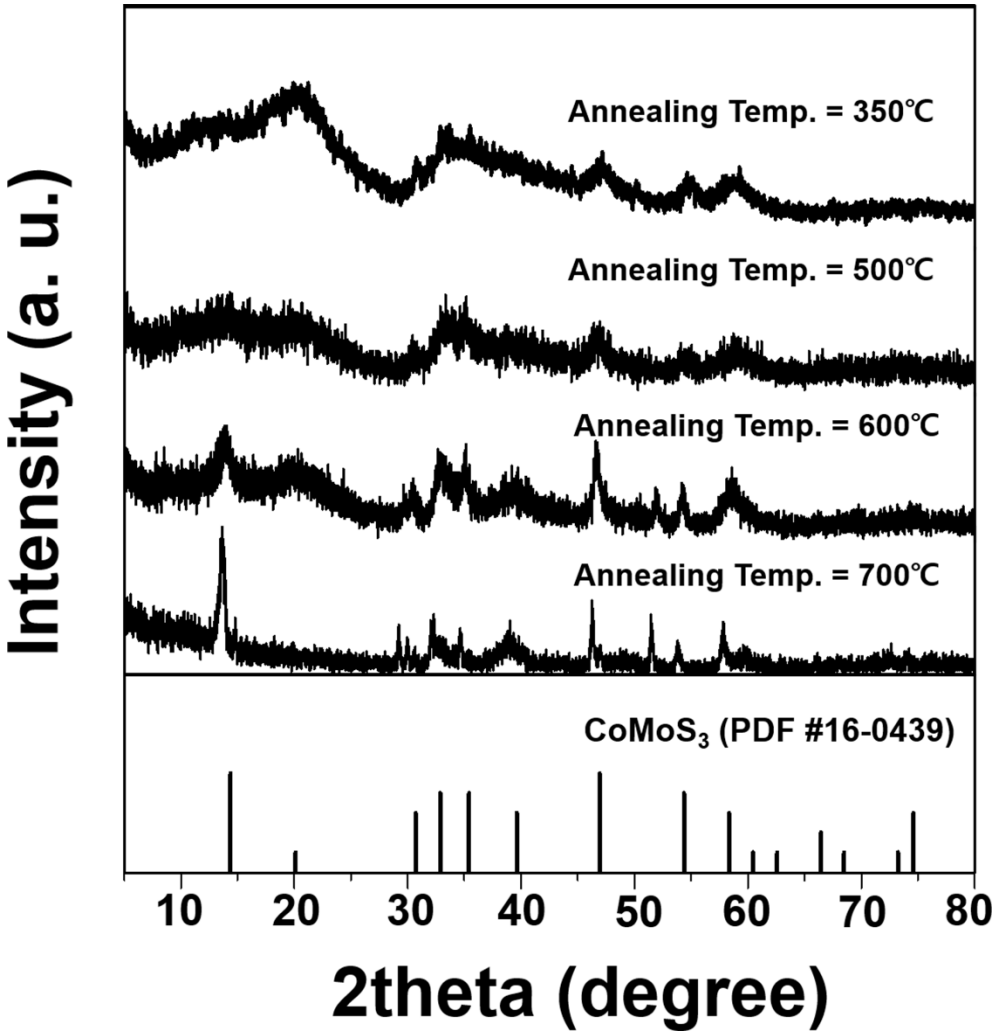

Fig. S1 XRD patterns of the $CoMoS_3$@NC annealed at temperatures of 350, 500, 600, and 700℃.

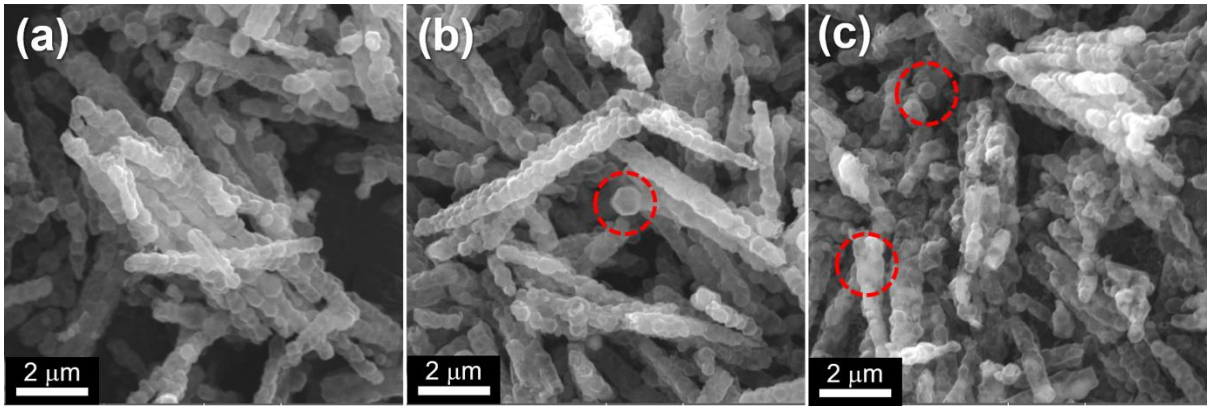

Fig. S2 Morphologies of $CoMoS_3$@NC annealed at temperatures of (a) 500, (b) 600, and (c) 700℃.

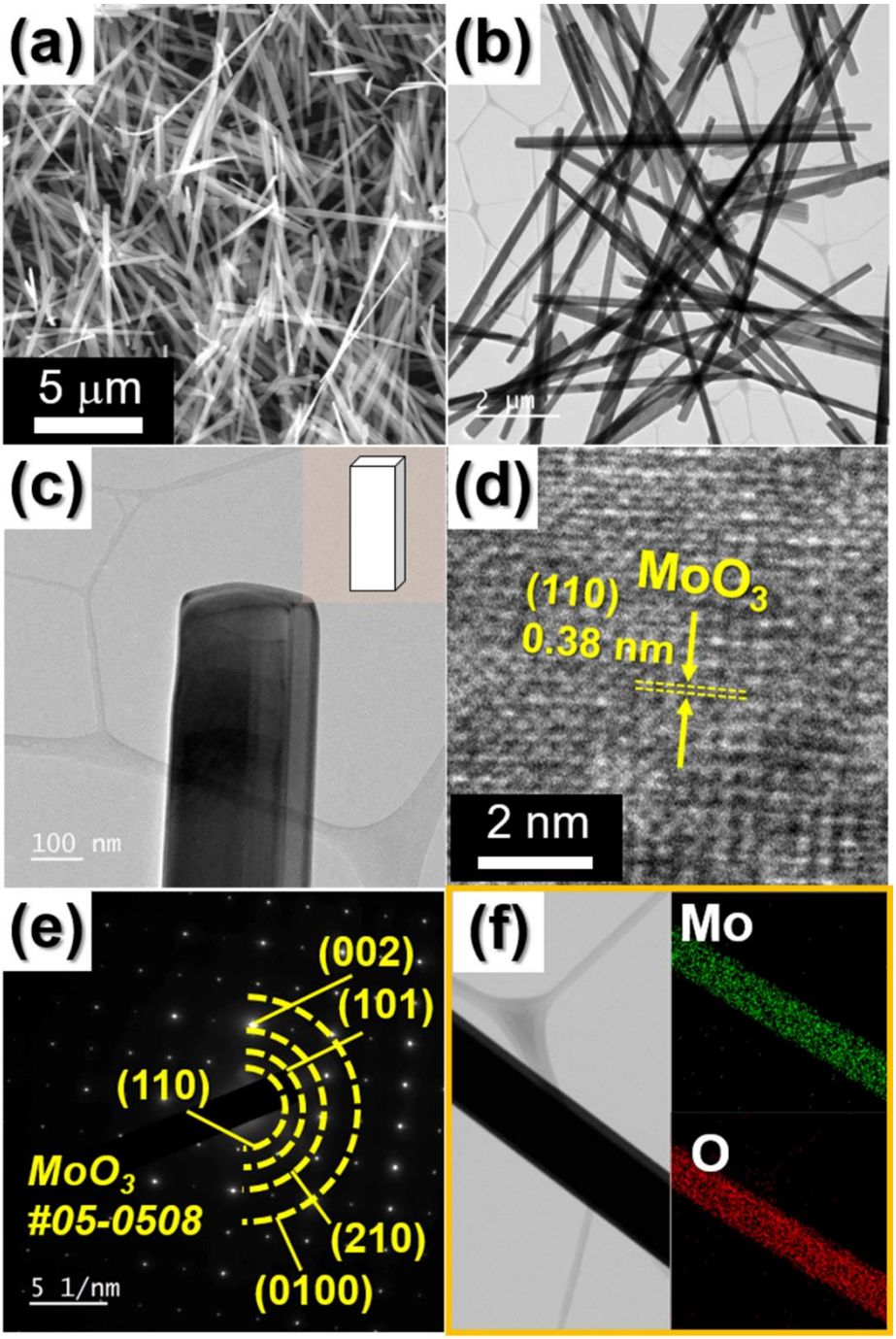

Fig. S3 Morphologies, SAED pattern, and elemental mapping images of MoO_3 nanobelt: (a) SEM image, (b,c) TEM images, (d) HR-TEM image, (e) SAED pattern, and (f) elemental mapping images.

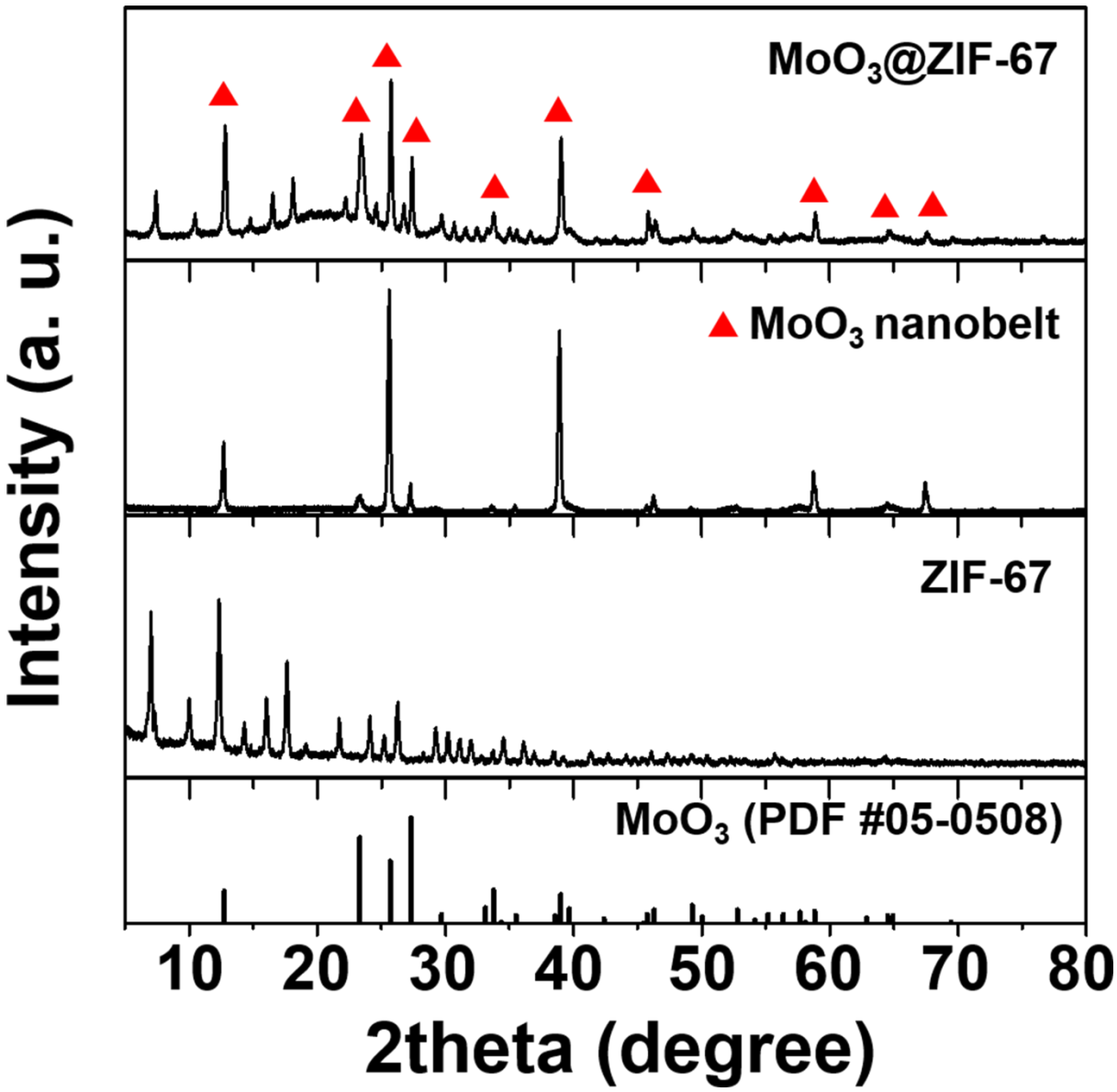

Fig. S4 XRD patterns of the MoO_3@ ZIF-67, MoO_3 nanobelt, and ZIF-67.

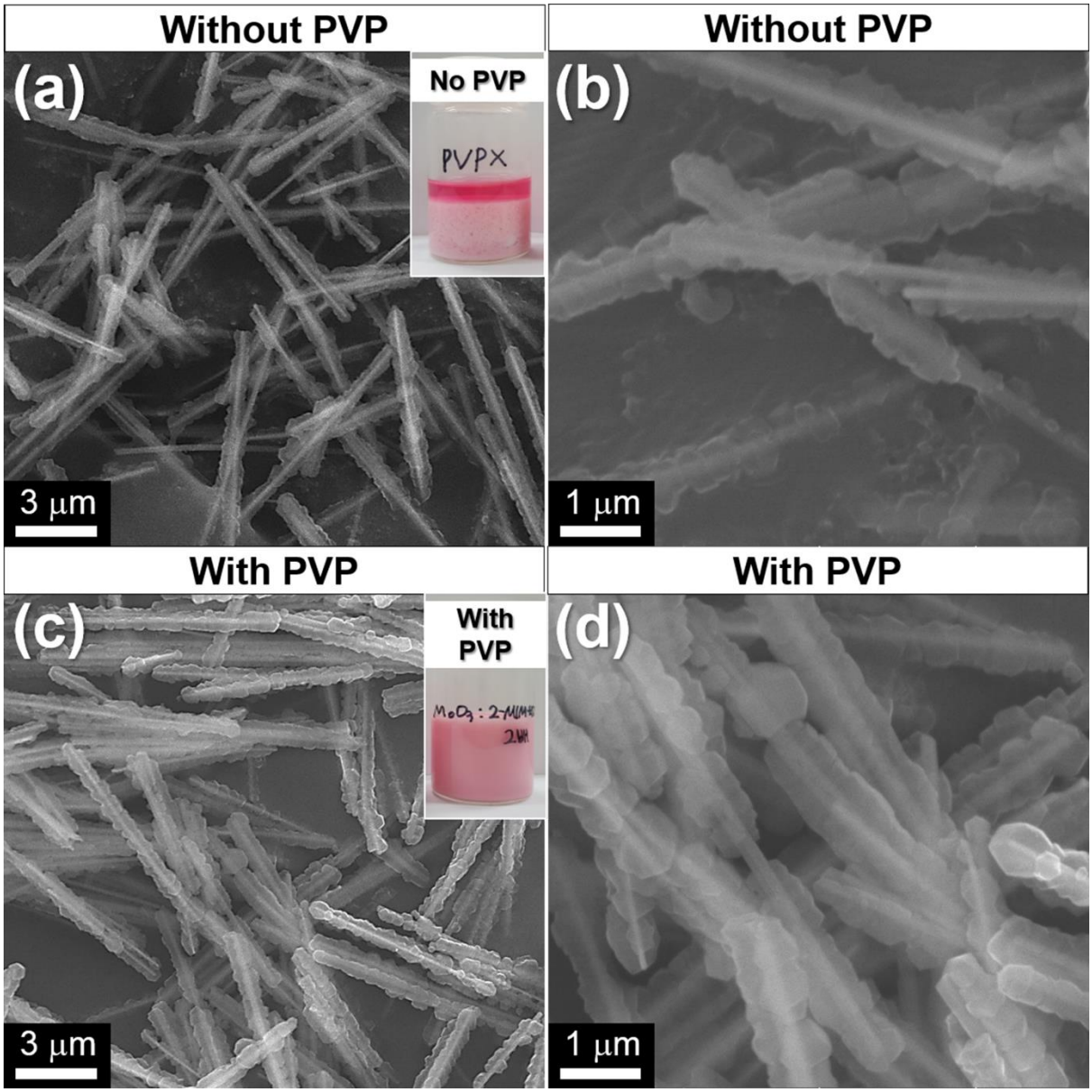

Fig. S5 Morphologies of MoO_3@ZIF-67 (a,b) without and (c,d) with PVP.

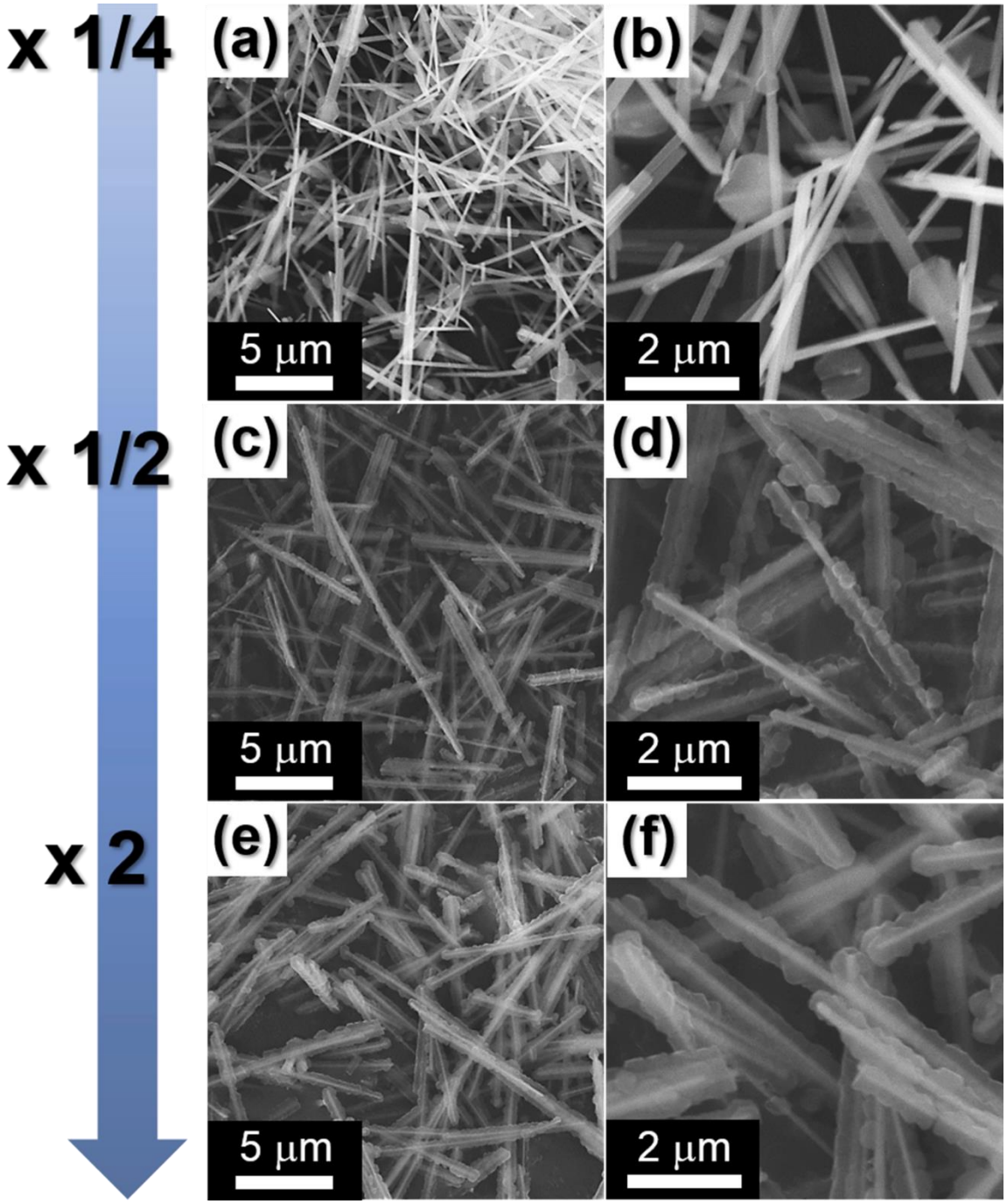

Fig. S6. Morphologies of MoO_3@ ZIF-67 formed from different amount of 2-MIM.

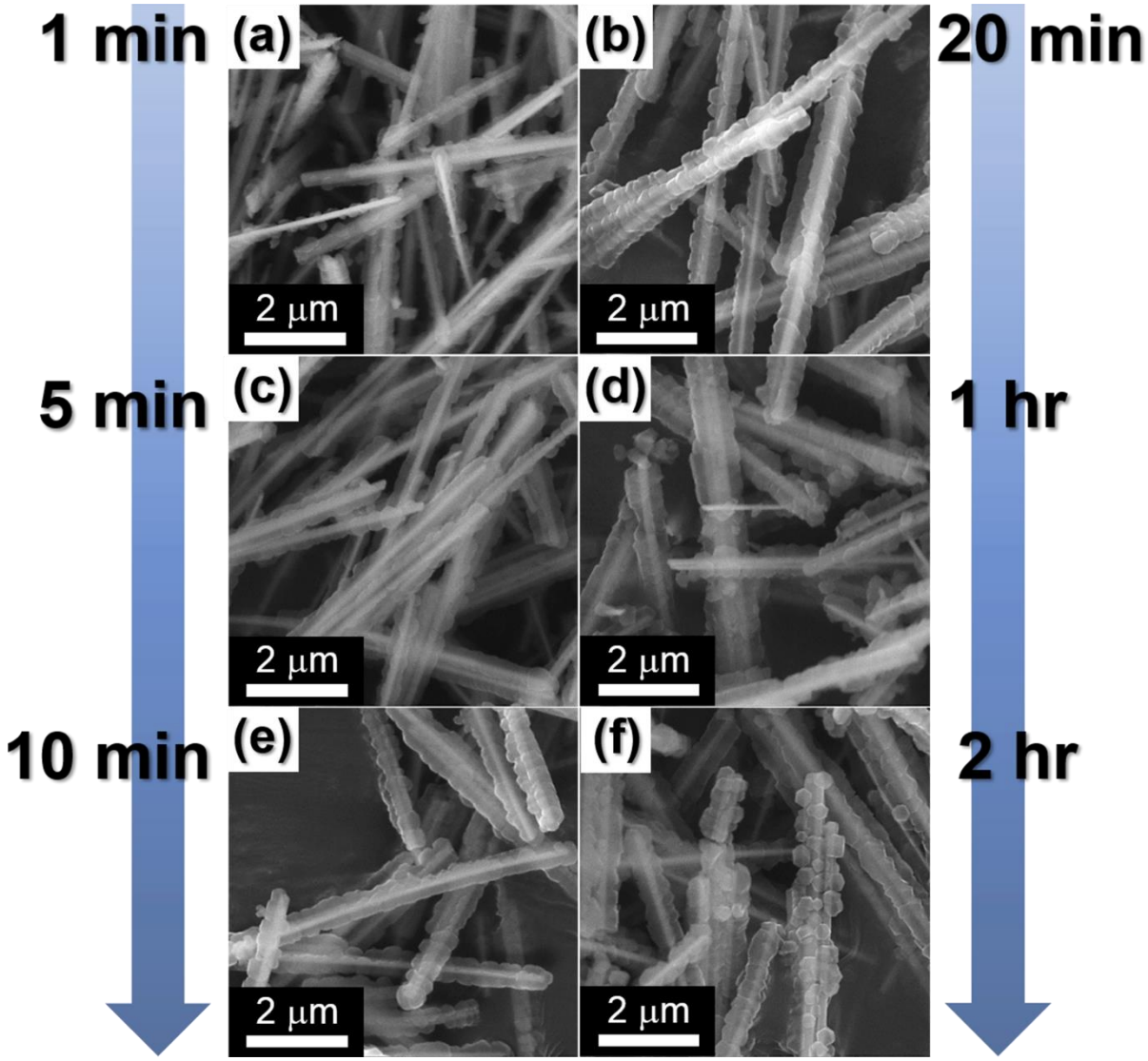

Fig. S7 Morphologies of MoO_3@ZIF-67 formed with different reaction times for ZIF-67 coating.

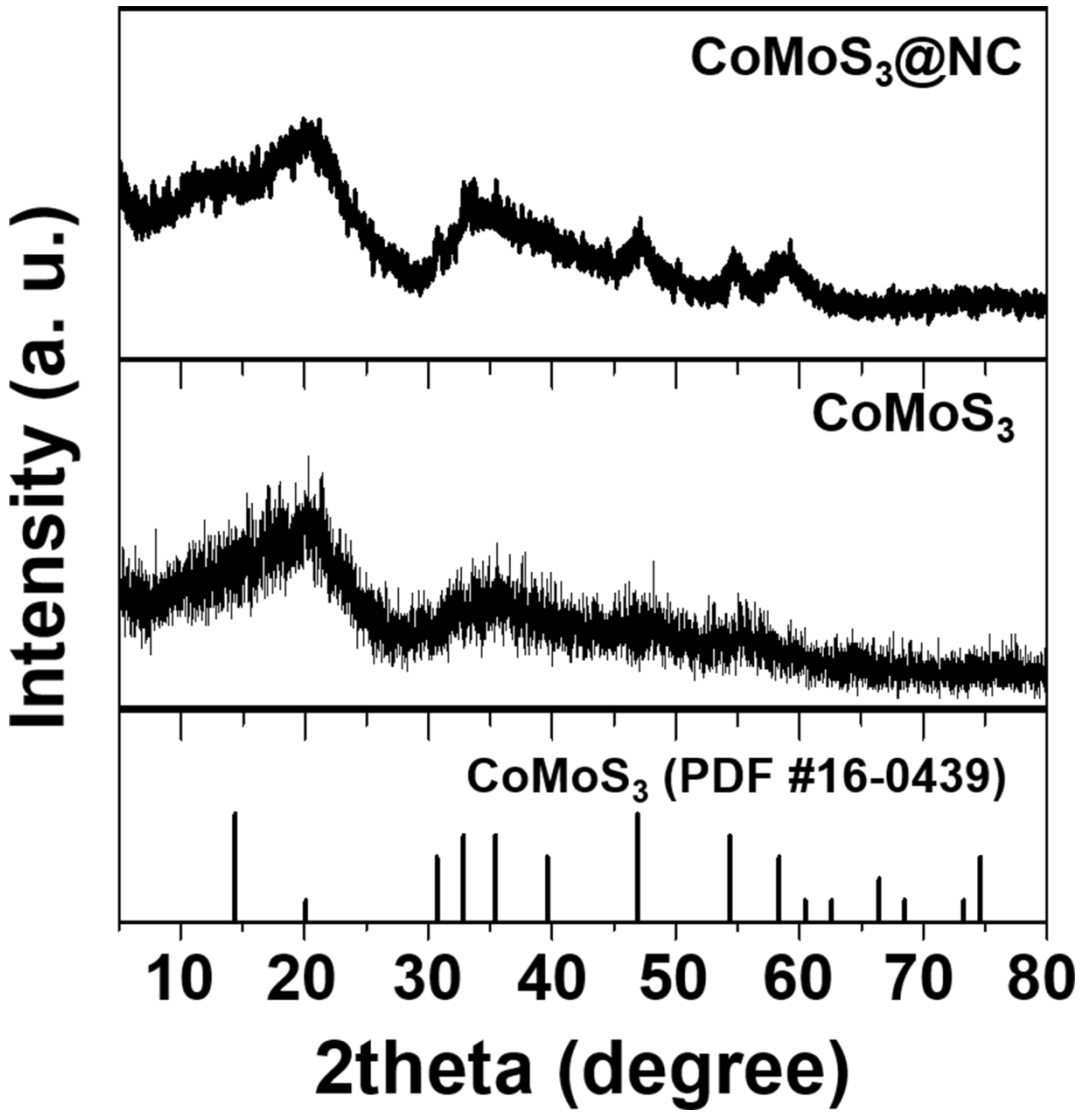

Fig. S8 XRD patterns of $CoMoS_3$@NC and $CoMoS_3$.

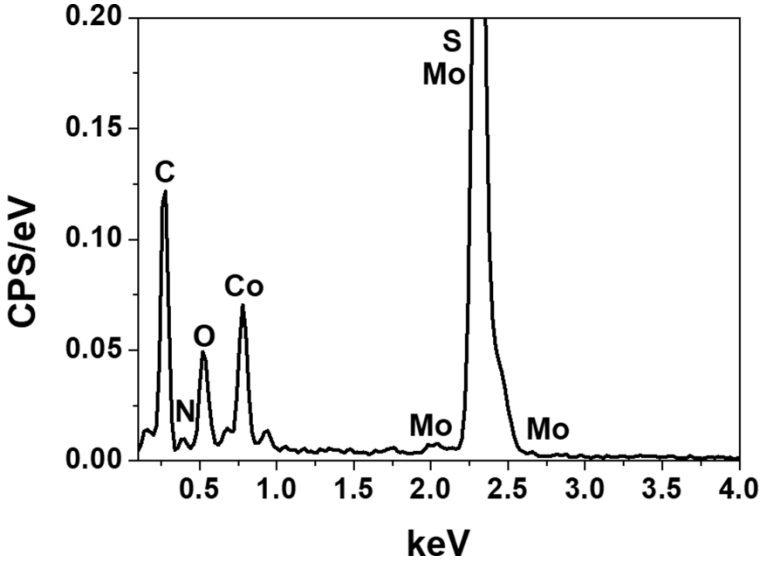

$CoMoS_3$@NC Nanobackbone		
Element	**wt%**	**at%**
C	24.1	51.3
S	32.9	26.4
N	0	0
O	5.9	9.5
Co	17.9	7.7
Mo	19.2	5.1
Total	100	100

Fig. S9 EDX measurement of $CoMoS_3$@NC.

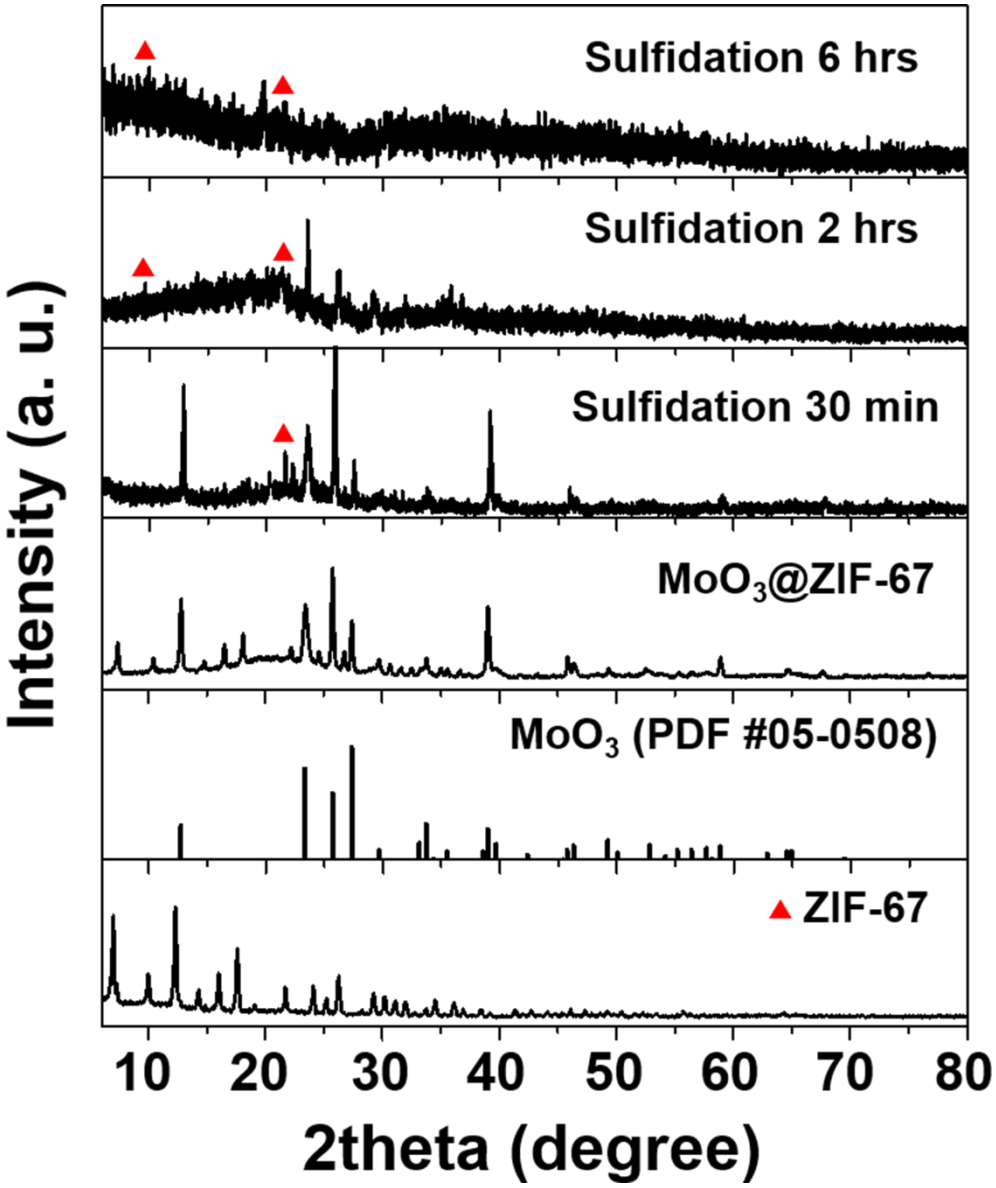

Fig. S10 XRD patterns of MoO_3@ZIF-67 obtained at various sulfidation times.

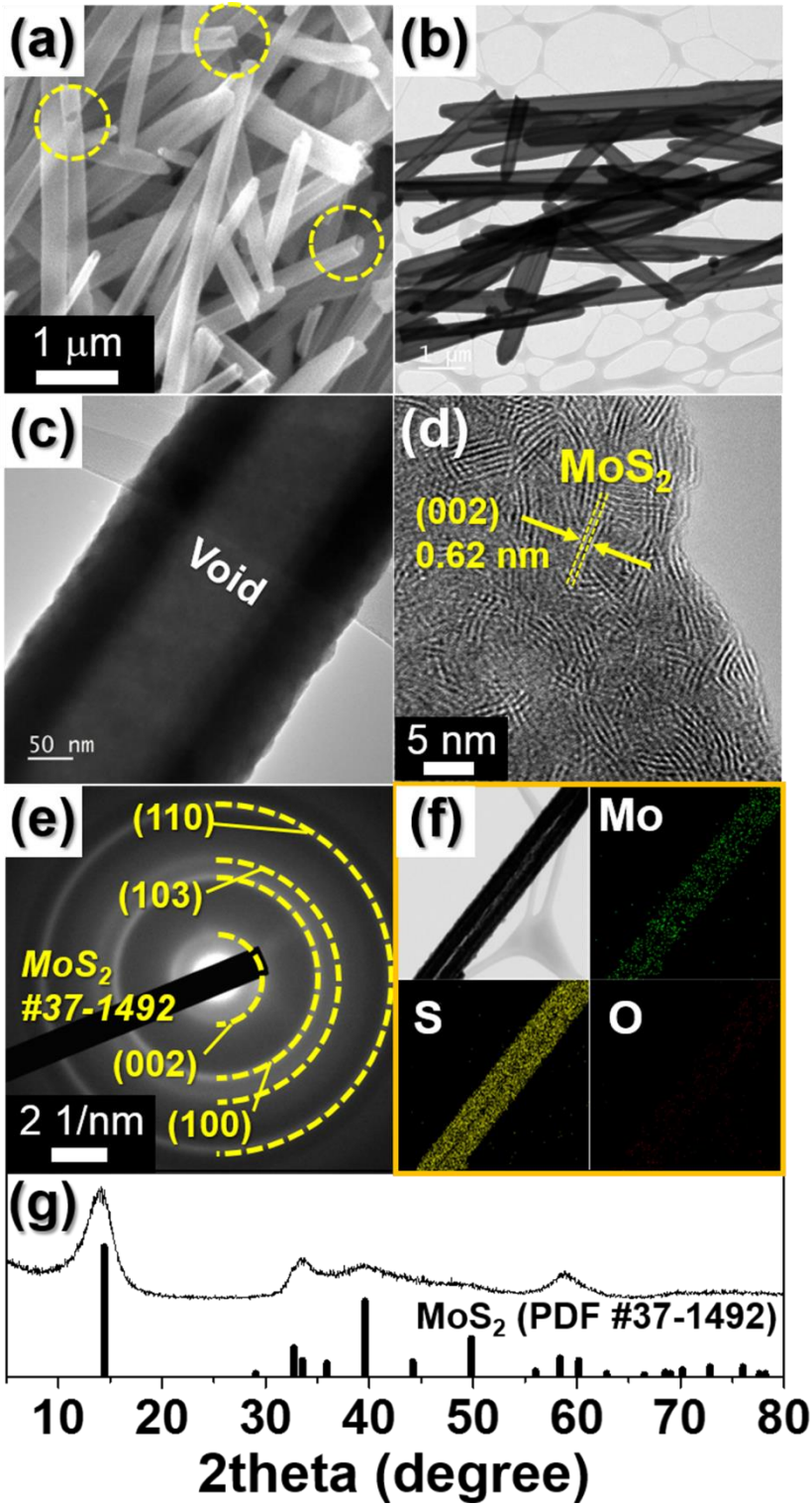

Fig. S11 Morphologies, SAED pattern, and elemental mapping images, XRD pattern of MoS_2 tube: (a) SEM image, (b,c) TEM images, (d) HR-TEM image, (e) SAED pattern, (f) elemental mapping images, and (g) XRD pattern.

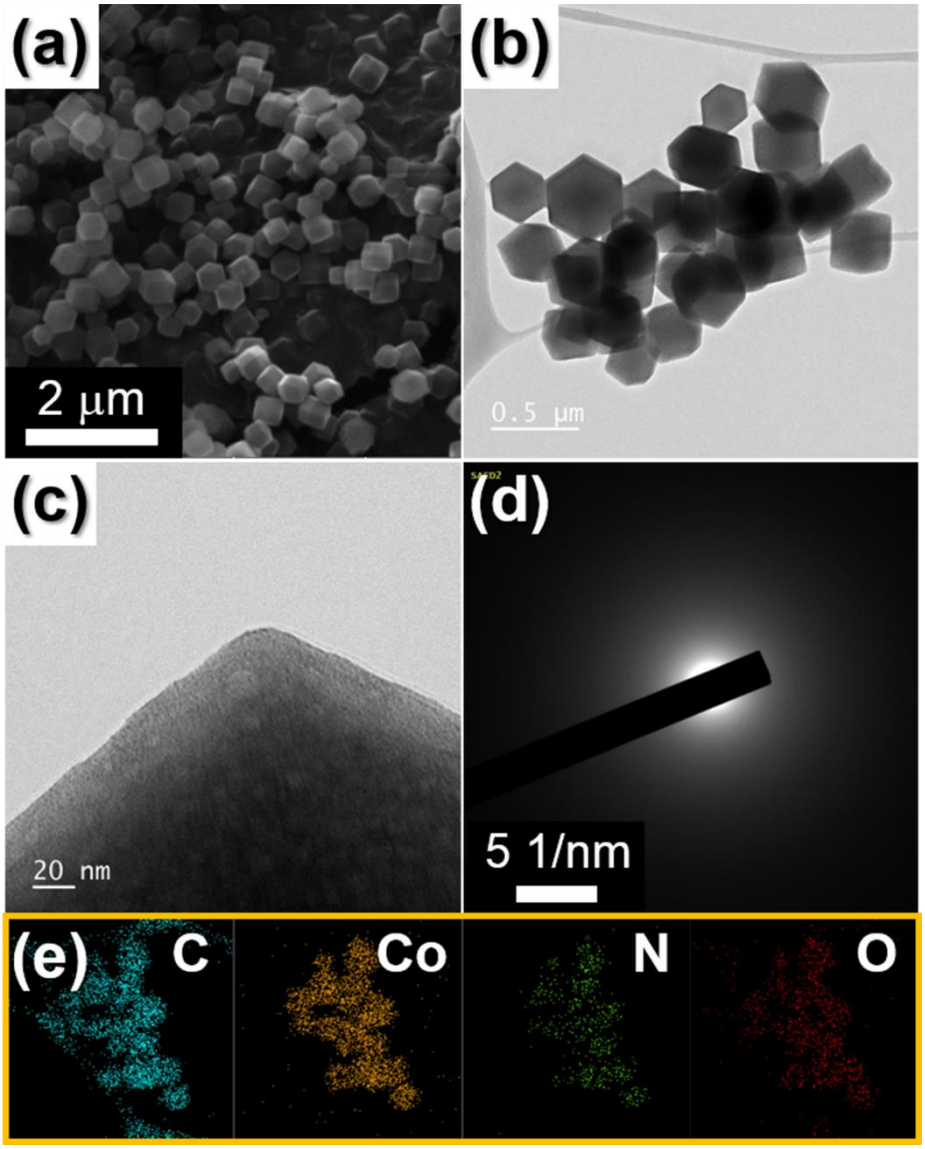

Fig. S12 Morphologies, SAED pattern, and elemental mapping images of ZIF-67: (a) SEM image, (b,c) TEM images, (d) SAED pattern, and (e) elemental mapping images.

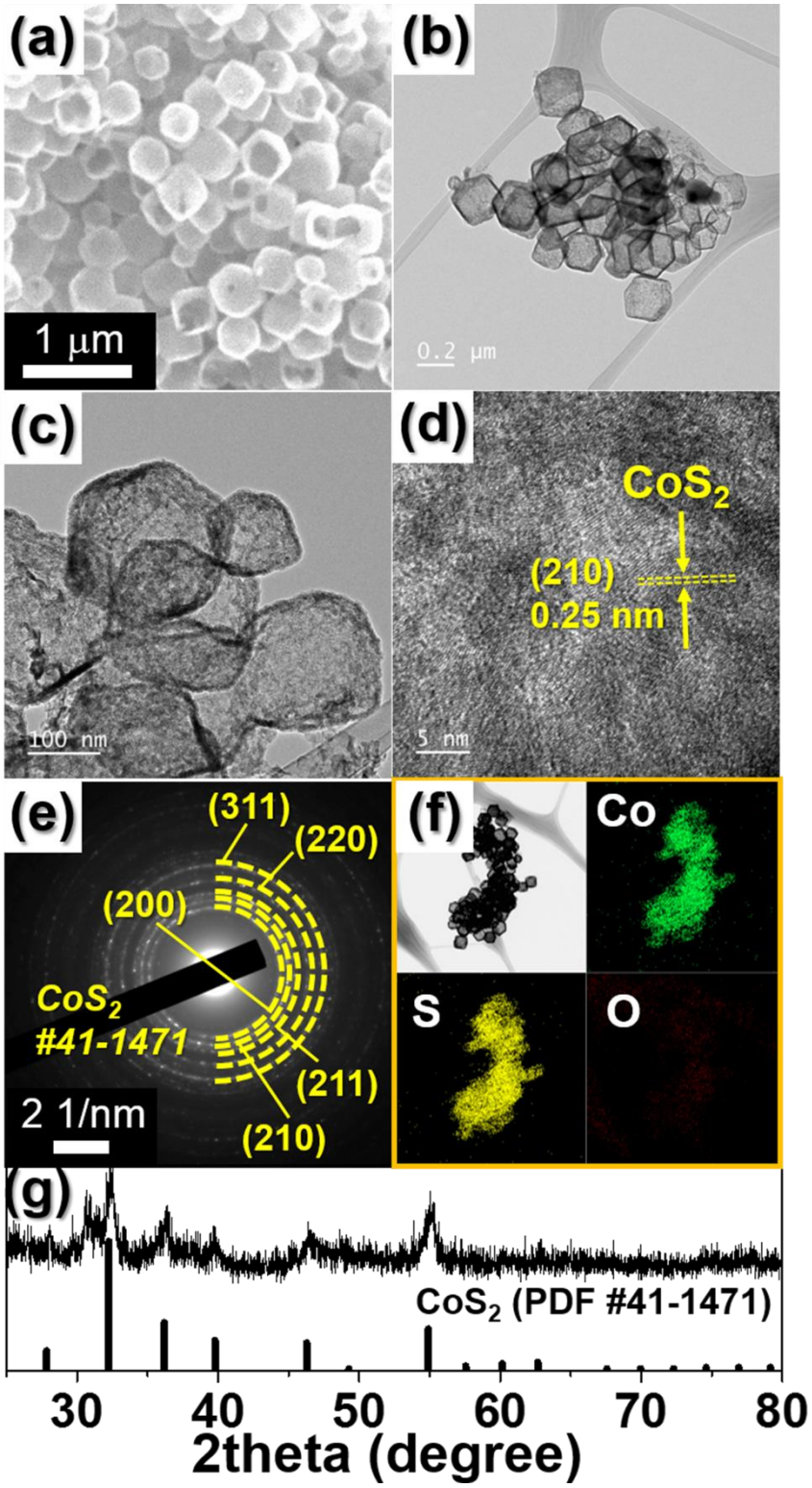

Fig. S13 Morphologies, SAED pattern, elemental mapping images, and XRD pattern of H-CoS_2: (a) SEM image, (b,c) TEM images, (d) HR-TEM image, (e) SAED pattern, (f) elemental mapping images, and (g) XRD pattern.

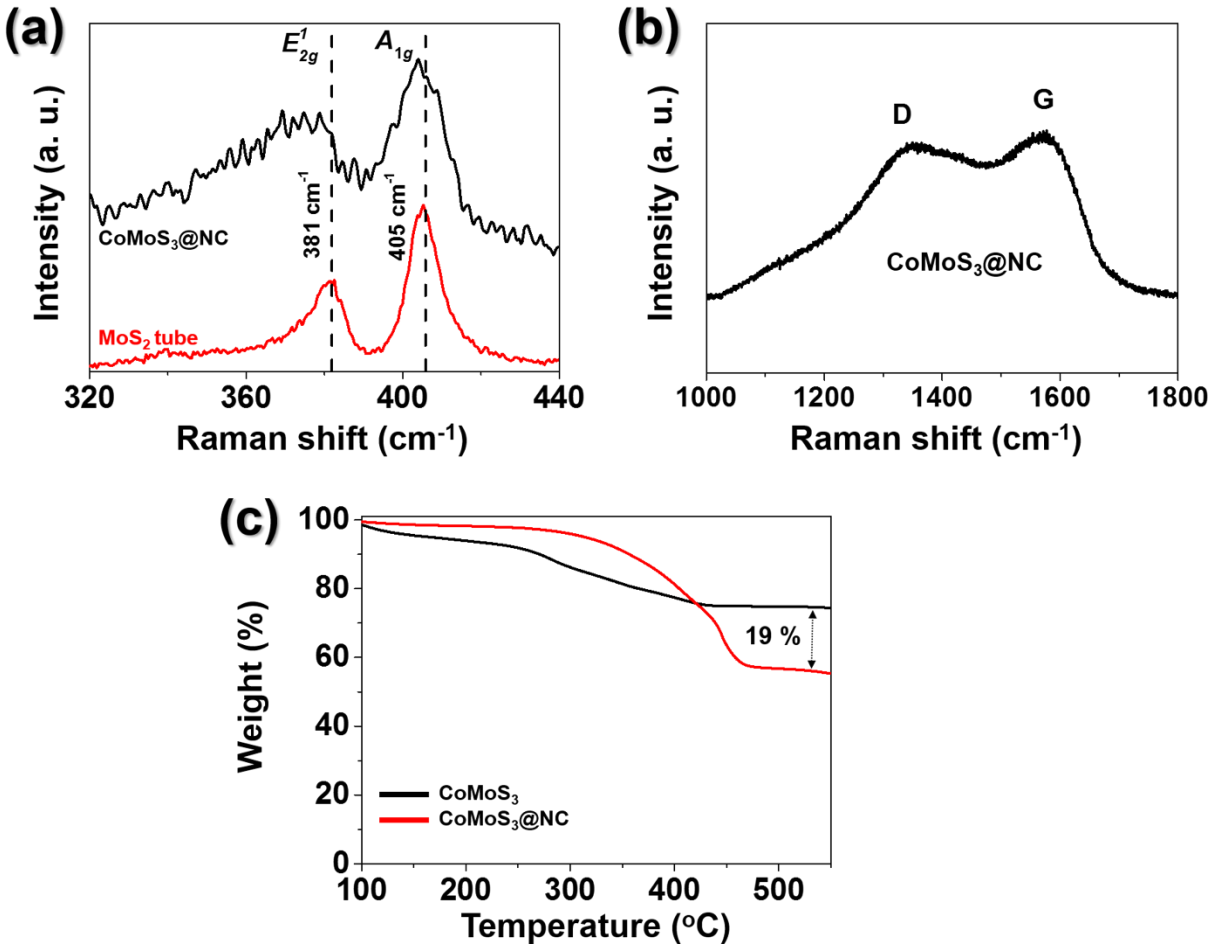

Fig. S14 (a) Raman spectra of $CoMoS_3$@NC and MoS_2 tube, (b) Raman spectra of $CoMoS_3$@NC, and (c) TGA curves of the $CoMoS_3$@NC and $CoMoS_3$.

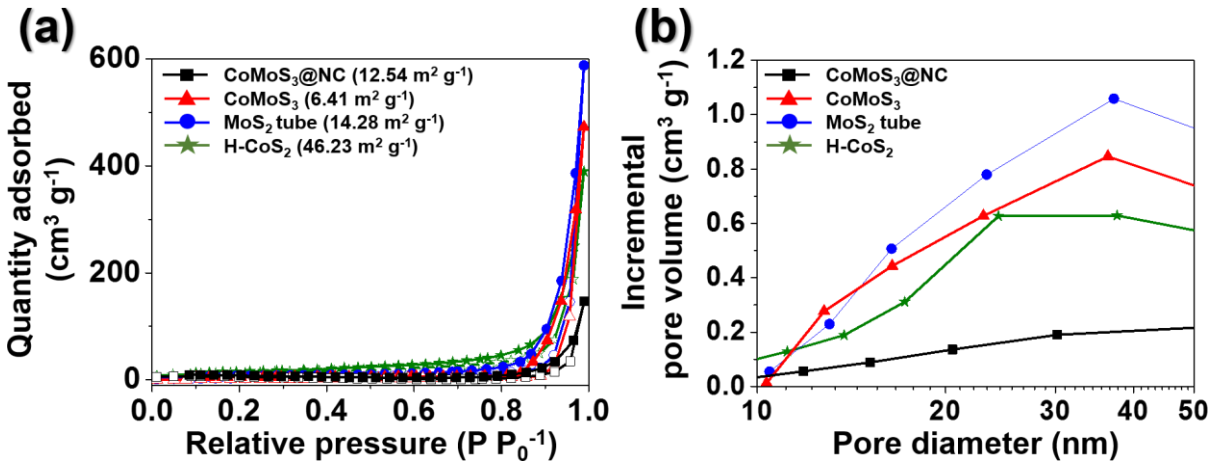

Fig. S15 (a) N_2 adsorption and desorption isotherms and (b) BJH pore size distributions of $CoMoS_3$@NC, $CoMoS_3$, MoS_2 tube, and H-CoS_2.

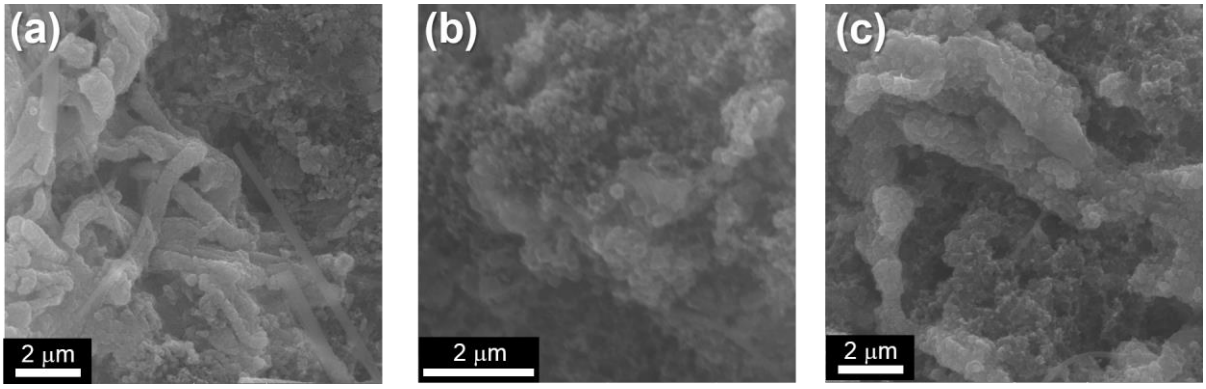

Fig. S16 Morphologies of (a) MoS_2 tubes, (b) H-CoS_2, and (c) $CoMoS_3$ after 100cycle.

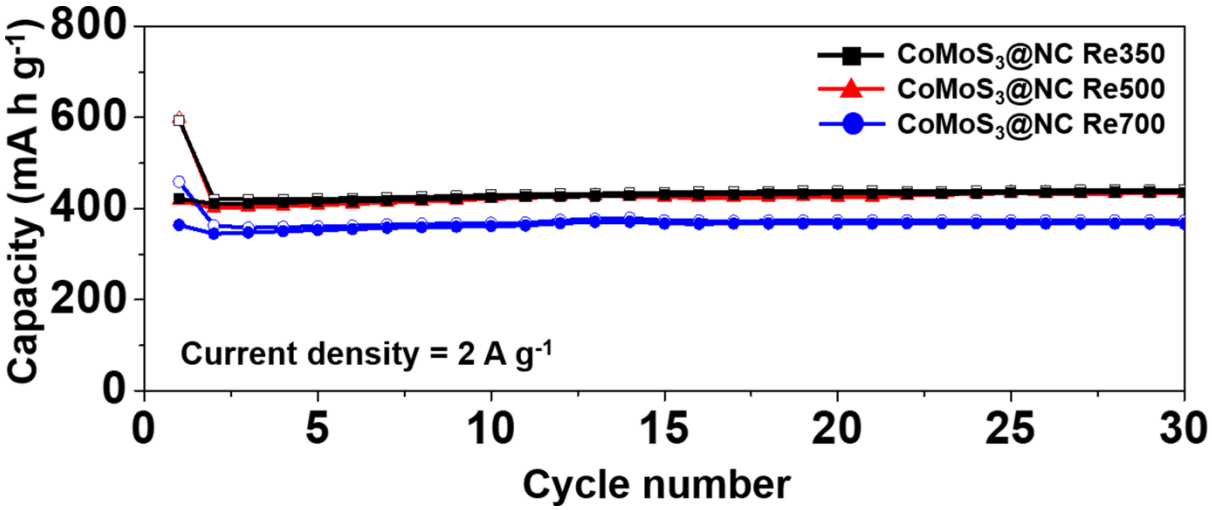

Fig. S17 Cycle performances of $CoMoS_3$@NC formed at different annealing temperatures at a current density of 2 A g^{-1}.

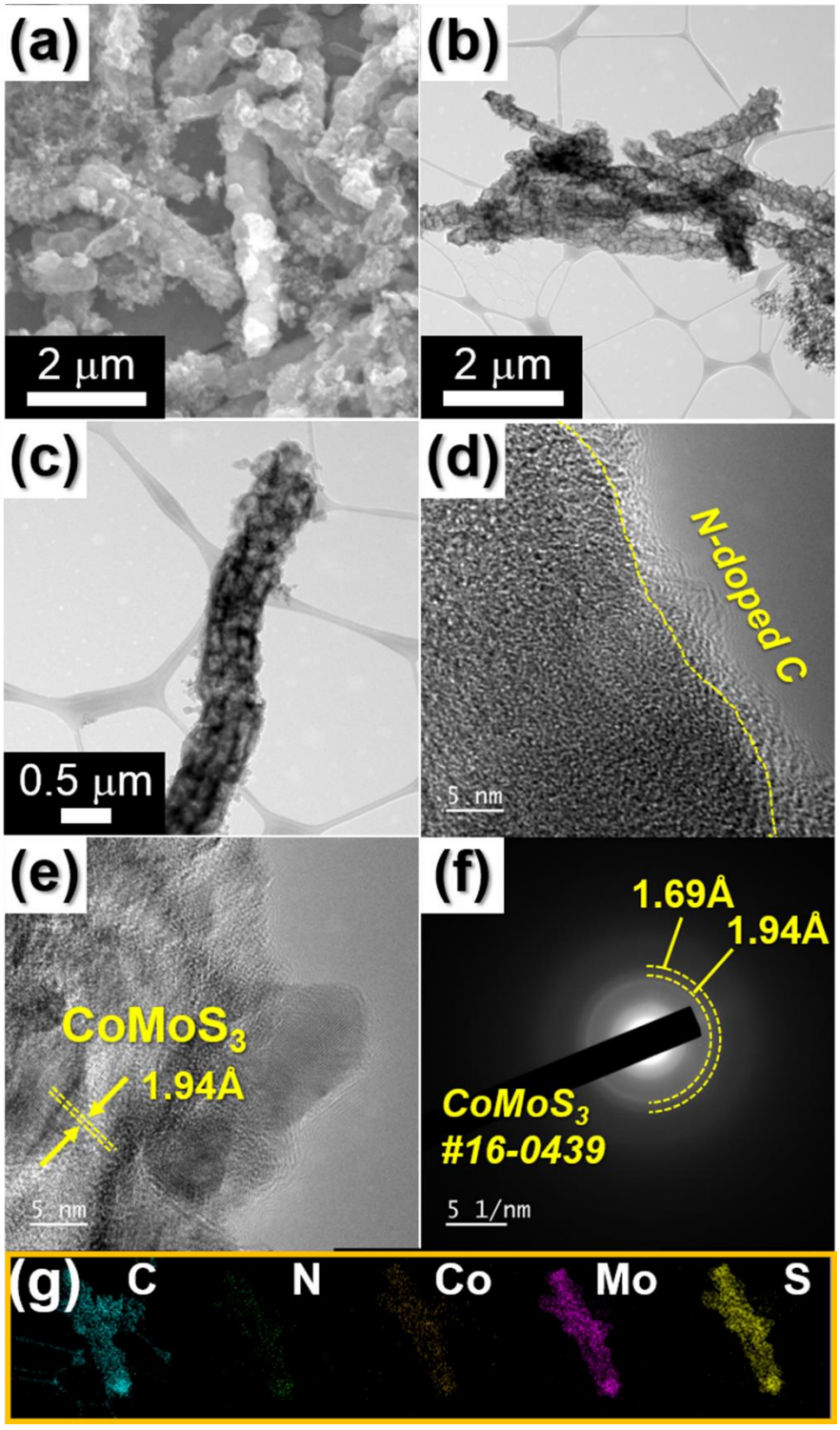

Fig. S18 Morphologies, SAED pattern, elemental mapping images of $CoMoS_3$@NC after 100cycle: (a) SEM image, (b,c) TEM images, (d-e) HR-TEM images, (f) SAED pattern, and (g) elemental mapping images.

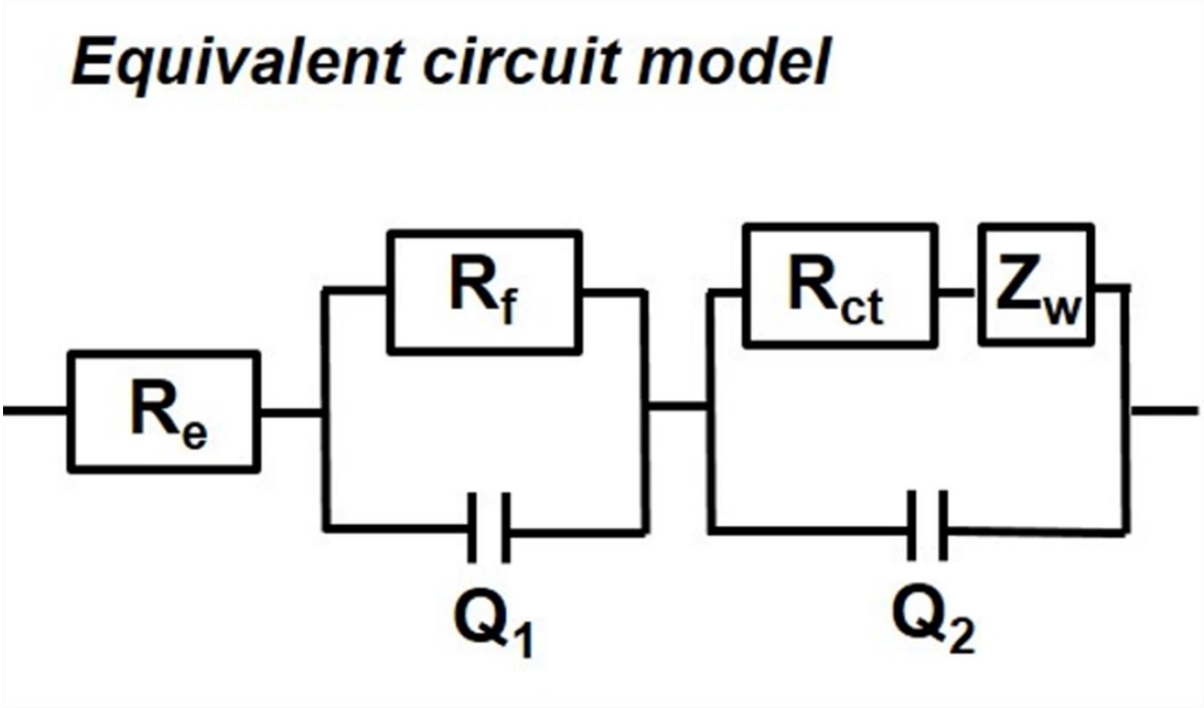

Fig. S19 Randle-type equivalent circuit model used for EIS fitting.

R_e: Electrolyte resistance, corresponding to the intercept of high frequency semicircle at Z_{re} axis

R_f: SEI layer resistance corresponding to the high-frequency semicircle

Q_1: Dielectric relaxation capacitance corresponding to the high-frequency semicircle

R_{ct}: Charge transfer resistance related to the middle-frequency semicircle

Q_2: Associated double-layer capacitance related to the middle-frequency semicircle

Z_w: Na-ion diffusion resistance

Table S1. C, H, O, and N contents in $CoMoS_3$@NC composite measured by EA analysis.

$CoMoS_3$@NC composite		
Element	**wt%**	**at%**
C	14.1	24.9
H	2.5	53.2
O	13.9	18.5
N	2.3	3.4

Table S2. Electrochemical properties of various Co-, Mo-, and CoMo sulfides materials applied as sodium-ion batteries reported in the previous literatures.

Material	Voltage range(V)	Current rate [mA g^{-1}]	Discharge capacity [mA h g^{-1}]	Cycle number	Initial Coulombic efficiency [%]	Capacity retention [%, from the 2nd cycle]	Rate capacity [mA h g^{-1}]	Loading mass of active material	Ref.
$CoMoS_3$ @NC	**0.001-3**	**500**	**478**	**200**	**77.7**	**83**	**349 (10.0 A g^{-1})**	**1.4 mg**	**Our work**
CoS_2/reduced graphene oxide	0.01-3	100	367	100	67	80	297 (1.0 A g^{-1})	1-1.2 mg	[S1]
MoS_2 nanosheets	0.01-3	40	386	100	~41	~57	251 (0.3 A g^{-1})	1.2 mg	[S2]
MoS_2/Co_9S_8/C	0.01-3	500	546	100	85	~79	222 (10 A g^{-1})	1.3-1.8 mg	[S3]
MoS_2@C nanotube composites	0.01-3	250	480	200	-	86	370 (2.5 A g^{-1})	1 mg	[S4]
Co_9S_8/MoS_2 yolk shell	0.01-3	300	476	100	50	90	403 (2.0 A g^{-1})	-	[S5]
Yolk-shell SnS-MoS_2	0.001-2.5	500	396	100	82	89	238 (7.0 A g^{-1})	1.4 mg	[S6]

Reference

[S1] K. Xie, L. Li, X. Deng, W. Zhou and Z. Shao, *J. Alloys Compd*., 2017, **726**, 394-402.
[S2] D. Su, S. Dou and G. Wang, *Adv. Energy Mater*., 2015, **5**, 1401205.
[S3] J. Xiang and T. Song, *Chem. Commun*., 2017, **53**, 10820-10823.
[S4] X. Zhang, X. Li, J. Liang, Y. Zhu and Y. Qian, *Small*, 2016, **12**, 2484-2491.
[S5] H. Geng, J. Yang, Z. Dai, Y. Zhang, Y. Zheng, H. Yu, H. wang, Z. Luo, Y. Guo, Y. Zhang, H. Fan, X. Wu, J. Zheng, Y. Yang, Q. Yan and H. Gu, *Small*, 2017, **13**, 1603490.
[S6] S. H. Choi and Y. C. Kang, *ACS Appl. Mater. Interfaces*, 2015, **7**, 24694-24702.